SPE 39746

Modeling Non-Equilibrium Mass Transfer Effects for a Gas Condensate Field

Wei-Jr. Wu, Peng Wang, Mojdeh Delshad, Chong Wang, Gary A. Pope and Mukul M. Sharma

Department of Petroleum and Geosystems Engineering, The University of Texas at Austin

Copyright 1998, Society of Petroleum Engineers, Inc.

This paper was prepared for presentation at the 1998 SPE Asia Pacific Conference on Integrated Modeling for Asset Management, 23-24 March 1998, Kuala Lumpur, Malaysia.

This paper was selected for presentation by an SPE Program Committee following review of information contained in an abstract submitted by the author(s). Contents of the paper, as presented, have not been reviewed by the Society of Petroleum Engineers and are subject to correction by the author(s). The material, as presented, does not necessarily reflect any position of the Society of Petroleum Engineers, its officers, or members. Papers presented at SPE meetings are subject to publication review by Editorial Committees of the Society of Petroleum Engineers. Electronic reproduction, distribution, or storage of any part of this paper for commercial purposes without the written consent of the Society of Petroleum Engineers is prohibited. Permission to reproduce in print is restricted to an abstract of not more than 300 words; illustrations may not be copied. The abstract must contain conspicuous acknowledgment of where and by whom the paper was presented. Write Librarian, SPE, P.O. Box 833836, Richardson, TX 75083-3836, U.S.A., fax 01-972-952-9435.

ABSTRACT

To assess the effect of non-equilibrium mass transfer on the productivity of a single well producing from a gas condensate field, a model incorporating non-equilibrium mass transfer effects was implemented into an equation-of-state (EOS) compositional reservoir simulator developed at The University of Texas at Austin.

A correlation from the literature was used to account for the effect of variables such as gas velocity and diffusion coefficients on the mass transfer coefficient. However, no mass transfer data were available for gas condensates, so a sensitivity study on the mass transfer coefficient was performed. Several simulations have been performed to evaluate the effects of the non-equilibrium mass transfer on the flow behavior in the region near the wellbore. The results from these runs were compared with those obtained under the local equilibrium assumption. Such comparisons reveal that non-equilibrium phase behavior lead to a reduction in the condensate saturation in the region near the wellbore. The mole fractions for light and heavy components in the oil phase are noticeably different. In the high velocity layers, these differences become more significant. In general, non-equilibrium effects lead to slower reductions in well productivity due to the fact that condensate dropout was reduced near the wellbore.

INTRODUCTION

Most reservoir simulation studies to date assume local equilibrium between the fluid phases. For high rate gas wells, the residence time for fluids in the gridblocks near wellbore is expected to be of the order of seconds. This is unlikely to provide sufficient time for the fluids to reach equilibrium with each other. Some laboratory experiments have supported this hypothesis (Burger *et al.*, 1996).

The purpose of this work is to assess the effect of the non-equilibrium mass transfer on the productivity of a single well producing from a gas condensate field. To do so, we have implemented a model dealing with non-equilibrium mass transfer into the equation-of-state (EOS) compositional reservoir simulator UTCOMP, developed at The University of Texas at Austin. This model is based upon data and correlation, published by Wilkins *et al.* (1995). To our knowledge, there are no data on mass transfer coefficients under high temperature and high-pressure gas condensate reservoir conditions. Therefor, we performed a sensitivity study on the mass transfer coefficient to assess the large uncertainty in it. Nghiem *et al.* (1997) recently presented a simulation study of dry gas displacing a light oil with mass transfer limitations and a constant mass transfer coefficient, but no comparisons with data were made. Burger and Mohanty (1997) studied the effect of diffusion on gas displacing oil, but each gridblock was assumed to be at local equilibrium, so this is not non-equilibrium mass transfer in the local sense.

Several simulations have been performed to evaluate the effects of the non-equilibrium mass transfer on the flow behavior in the region near the wellbore. The dependence of relative permeability and residual saturations on the capillary number was not used so that we could assess just this one effect, but in future simulations the combined effects should be included since separate studies have shown that capillary number effects can be very large under these conditions. The results from these simulations were compared with those obtained under the local equilibrium assumption.

THE UTCOMP SIMULATOR

The UTCOMP simulator is a three-dimensional, EOS compositional reservoir simulator (Chang *et al.*, 1990). The formulation follows the one by Acs *et al.* (1985) with some changes. The solution scheme is analogous to IMPEC (implicit pressure and explicit composition). A higher-order finite-difference method with the total variation diminishing

(TVD) scheme as well as the conventional one-point upstream weighting method is available to discretize the partial differential component-mass-balance equation. Three-phase flash calculation is also implemented so that UTCOMP is capable of modeling four-phase flow. Both Peng-Robinson (PR) EOS (Peng and Robinson, 1976) and the modified Redlich-Kwong by Turek *et al.* (1984) can be used for phase-behavior calculations. Relative permeability can be treated as a function of interfacial tension and velocity through the capillary number. Tracers, surfactant, foam and polymer effects can also be modeled with UTCOMP.

NON-EQUILIBRIUM MASS TRANSFER MODEL

The non-equilibrium mass transfer model of Wilkins *et al.* (1995) is as follows:

$$J_i a_0 = k_{0i}(C_i^{eq} - C_i) \tag{1}$$

where J_i is the mass flux; a_0 is the specific interfacial area; k_{0i} is the mass transfer coefficient of a component i; and C_i is the concentration of component i in the flowing phase. The coefficient k_{0i} was evaluated using packed bed experiments. The superscript eq means the corresponding property is evaluated at equilibrium.

When the mole fraction of each species in the gas is used in place of the mass concentration, Eq. (1) becomes:

$$\frac{\partial x_{ig}}{\partial t} = k_{0i}(x_{ig}^{eq} - x_{ig}) \tag{2}$$

where x_{ig} is the mole fraction of component i in the gas phase; and x_{ig}^{eq} is the mole fraction of component i in the gas phase at equilibrium.

The coefficient k_{0i} in Eq. (2) is the mass transfer coefficient for component i in the gas phase and is computed using the following correlation by Wilkins *et al.* (1995):

$$k_{0,i} = m d_{50}^{0.44} V_g^{0.62} D_{i,g}^{0.38} \tag{3}$$

where m = 0.38 in $1/cm^{1.82}$; d_{50} is the mean grain size in cm; V_g is the gas interstitial velocity in cm/sec; and $D_{i,g}$ is the diffusion coefficient of component i in the gas phase in cm^2/sec.

The constant m is treated as an input to the UTCOMP simulator. A sensitivity study was performed by varying the value of m. The mass transfer coefficient, k_{0i}, has units of 1/sec. For the calculation of the mean grain size, d_{50}, the Carman-Kozeny correlation (Carman, 1937) was used:

$$d_{50} = \left(\frac{ck(1-\phi)^2}{\phi^3} \right)^{0.5} \tag{4}$$

In Eq. (4), k is the rock permeability in cm^2 and ϕ is the rock porosity. The computed values of d_{50} in each gridblock instead of the average values are used in this work. The constant c in Eq. (4) is assumed to be 300 (Wilkins *et al.*, 1995).

Using the finite difference scheme, Eq. (2) becomes:

$$x_{i,g}^{n+1} = x_{i,g}^{n} + \Delta t\, k_{o,i} \left[\left(x_{i,g}^{eq} \right)^{n+1} - x_{i,g}^{n} \right] \tag{5}$$

Using Eq (5), the mole fraction of each component can be calculated at a new time step. Then, the EOS parameters are updated using the new composition. The phase properties also need to be recalculated.

UTCOMP SOLUTION PROCEDURE FOR THE NON-EQUILIBRIUM MASS TRANSFER OPTION

The IMPEC nature and the volume-balanced formulation of the UTCOMP simulator make extensions of its capability not as complicated as other simulators. The procedure we implemented was to use Eq.(5) to correct the equilibrium phase composition. The calculation at one timestep may be outlined as follows:

1. compute coefficients of pressure equation and solve pressure equation implicitly;
2. compute total number of moles for each component in each gridblock using component mass balance equation;
3. perform equilibrium calculation (flash) to determine number and saturation of phases and composition for each separate phase in each gridblock using new pressure;
4. account for non-equilibrium mass transfer effects using Eq. (5) for gas phase;
5. re-compute oil-phase saturation and composition using a molar balance calculation;
6. update rock and phase properties and phase relative permeability using new phase saturation and composition;
7. go to next timestep.

It can be seen that Steps 4 and 5 are added for this option.

FLUID DESCRIPTION

The PR EOS is used to compute equilibrium mass transfer for hydrocarbon components and phase volumes. In developing the model for the gas condensate examined, we employed the procedure suggested by Wang *et al.*, 1997. which includes the following steps:

- select a fluid sample representative of the actual gas condensate where experimental PVT data is available;
- describe the heavy end of the fluid sample using as many as 44 different methods (combinations of different methods in each step of the characterization procedure);
- choose a base fluid description that can best predict experimental liquid dropout data of a constant-volume depletion (CVD) process for water-free sample;
- perform fine-tuning of critical properties of the heavy pseudocomponents of the base fluid description to match measured CVD data of water-free sample;

- test predictive capability of the model by applying it to predict phase behavior of both water-free and water-containing samples.

Based on the above procedure, a fluid sample that shows a relatively high liquid dropout (around 1.5%) at a temperature of 353°F was chosen as the reference fluid. Among the 44 fluid descriptions tried, the one using

1. the exponential function to split C_{7+} fraction into 45 pseudocomponents;
2. the Gaussian quadrature method to lump the split components into two heavy groups;
3. the TWU correlation (Twu, 1984) to compute the critical properties and acentric factors of each pseudocomponent; and
4. two pseudocomponents to represent components between ethane and hexane,

was found to reasonably predict experimental dewpoint pressure and CVD liquid dropout data of the reference fluid. After fine-tuning, a 6-component PR EOS model for water-free fluid was developed, whose composition and properties for each component are listed in Table 1. Figure 1 shows the liquid dropout curve obtained from this model, which is in satisfactory agreement with experimental data. Additionally, this model can

- estimate satisfactorily the Z-factor of both dry and wet samples, which are shown in Figures 2 and 3 respectively; and
- predict acceptable shape of pressure-temperature phase envelop (Figure 4).

It should be added that models developed from other fluid-description procedures predicted an un-closed shape of the phase envelop. Figure 5 shows a typical prediction for the phase envelop using such procedures.

It was found that the volume-shift parameters are not necessarily needed in order to match the PVT data for this gas condensate.

DIFFUSION COEFFICIENTS

The diffusion coefficients for each component in the gas phase were calculated using the correlation of Wilke and Lee (1955). For the components in the liquid phase, the diffusion coefficient correlation of Wilke and Chang (1955) was used. A detailed description of these correlations is given in Appendix A. Some component physical properties required by these correlations are taken from the reference book of Reid *et al.* (1987). Table 2 presents the diffusion coefficients used in our simulations, which are similar to the values used in the study of Burger and Mohanty (1997).

RESERVOIR DESCRIPTION AND SIMULATION SPECIFICATIONS

The simulation input was based partly on the description and data for the Arun field given in the paper by Afidick *et al.* (1994). In order to estimate non-equilibrium effects on well productivity, radial flow into a single well was simulated using a two-dimensional x-z cross section with an angle of 36° (a pie shape as shown in Fig. 6). The simulation grid has 8 layers in the vertical direction with the highest permeability layer at the top (layer 1) and the lowest permeability at the bottom (layer 8). The horizontal permeability for each layer is listed in Table 3. The grid has nineteen gridblocks in the x direction that vary between 1 ft near the well and 500 ft farthest from the well.

The reservoir temperature is 335 °F. The initial pressure is 4100 psi, which is in the retrograde condensate region. The critical condensate saturation was 0.25. The residual saturations for water and gas were 0.30 and 0.375, respectively.

Corey's model was used to compute relative permeability. The parameters for this model were obtained by matching the experimental data from Henderson *et al.* (1997). The endpoint relative permeability for gas and oil were 0.53 and 0.05 and the exponents for gas and oil were 2.3 and 5.8, respectively. These values correspond to low capillary number conditions and were not varied during these simulations.

The production rate for the entire well is 44 x 10^6 SCF/day. In our simulations, only one tenth of this rate was specified because we were simulating a pie shape with only 36 degrees. Further, we assumed that the well penetrates the entire eight layers. The production rate is allocated to each layer based on the phase mobility (a ratio of the phase relative permeability to its viscosity) of the gridblock containing the well. An open boundary with a constant pressure of 4100 psi is used for the outer boundary of the reservoir, which allows the fluid having the initial composition to flow into the simulation domain.

Simulations were performed using the mass transfer coefficient proposed by Wilkins *et al.* (1995). This correlation was developed based on experimental data under low pressure and temperature conditions. The variables in the correlation include gas-phase interstitial velocity, diffusion coefficient for each component and mean grain size of the sand.

Several simulations using the UTCOMP simulator with the above mentioned specifications have been performed. Since no gas condensate experimental data are available to compare with, simulations were conducted based on the variation of the constant m in Eq. (3). We used 0.38, 0.038, and 38 for this constant.

RESULTS AND DISCUSSION

Figures 7 and 8 show the oil saturation profile in layer 1 (high permeability layer) after 10 and 30 days. Non-equilibrium mass transfer leads to a reduction of the condensate saturation in the region near the wellbore compared to local equilibrium. The saturation difference at 30 days ranged between 4% to 33% for the case with m=0.38. This reduction in the condensate saturation increases as the non-equilibrium mass transfer coefficient decreases. For the case with m=38, the simulation results are almost the same as the local equilibrium results. Similar results were also observed for layers 3 and 8 (Figs. 9 and 10), which have relatively low permeability.

The differences in the pressure profiles (Figs. 11 and 12) and well productivities are not significant largely because the condensate saturation was too low to flow in all cases (note again that a fixed residual condensate saturation of 0.25 was used in these three simulations). For simplicity, the effect of capillary number was not included in these simulations. In

other simulations, we have found significant reductions in condensate saturation near the well due to the very high capillary numbers near the well.

Figure 13 shows the velocity as a function of distance in layers 1 and 8 after a period of 30 days. Figure 14 illustrates the mass transfer coefficients for the lightest component, methane, and the heaviest component, C_{11}^{+}, corresponding to the velocity profiles plotted in Figure 13 and the diffusion coefficient listed in Table 2. The lighter components achieve equilibrium relatively faster than the heavier components. The nonequilibrium calculations include both the mass transfer coefficient and the magnitude of the driving force due to the mole fraction difference between local equilibrium and flowing mole fractions. These calculations are coupled since the driving force is a function of pressure and thus the phase behavior. Figures 15 and 16 show a significant effect on the component concentration in the condensate phase but not in the gas phase for all the components except for the heaviest component of C_{11}^{+}. The term deviation in these figures means the ratio of the difference in component mole fraction between equilibrium and nonequilibrium cases to the component mole fraction from the equilibrium case. An increase in concentration of heavy components in the oil phase near the wellbore causes an increase in the specific gravity and viscosity of the oleic phase. This can reduce the transmissibility of the oleic phase, which also helps explain the results in Figures 15 and 16. In the gas phase, the mole fraction of the heaviest component is 1.8×10^{-3} compared to the 1.3×10^{-3} of the equilibrium case. Thus, the effect of component deviation in the gas-phase properties would not be large.

To further study these phenomena, a simulation with dry gas injection from the outer boundary was performed. The injection well was kept at a constant bottomhole pressure of 4100 psi. The composition of the injected gas is listed in Table 4. Figures 17 and 18 show the saturation and pressure distributions of the oil phase for the cases with and without nonequilibrium mass transfer. Similar trends are observed compared to the previous results with the open boundary. These results indicated that the effect of nonequilibrium mass transfer on the productivity index is not significant. Figures 19 and 20 show the effect of non-equilibrium mass transfer on the component distribution.

SUMMARY AND CONCLUSIONS

A simulation study of the effect of non-equilibrium mass transfer on the well productivity of a gas condensate well has been performed using an EOS compositional reservoir simulator that includes a correlation of the mass transfer coefficient taken from the experimental literature. From these simulation results, we observed the following:

•the non-equilibrium phase behavior leads to a reduction in the condensate saturation in the region near the wellbore

•the mole fractions for both the light and heavy components in the oil phase are noticeably different when the mass transfer is not instantaneous. In the high velocity layers, the differences are more significant

These results suggest that non-equilibrium mass transfer might be important under some conditions of very high flow rate wells and thus merits further research. There is a need to measure mass transfer coefficients for gas condensates to either verify the available mass transfer coefficient correlation or develop a new correlation. Also, the effects of capillary number and diffusive flux should be included in future studies and more understanding of how mass transfer effects might interact with formation heterogeneity and non-Darcy flow in high rate gas condensate wells is needed.

ACKNOWLEDGMENTS

We thank Kathy Hartman, Ravi Vaidya, Mary Coles and Myung Hwang of Mobil Exploration and Production Technical Center (Meptec) for useful discussions and funding this research.

NOMENCLATURE

a_0	specific interfacial area, cm^2
C	concentration of solute in the flowing phase, volume faction
$D_{i,g}$	diffusion coefficient of component i in gas phase in cm^2/sec
d_{50}	mean grain size, cm
J	mass flux, $g/cm^2/sec$
k	rock permeability, cm^2
k_0	mass transfer coefficient , 1/sec
V_g	gas interstitial velocity, cm/sec
$x_{i,g}$	mole fraction of component i in gas phase
$x_{i,g}^{eq}$	mole fraction of component i in gas phase at equilibrium.

REFERENCE

Acs, G., Doleschall, S., and Farkas, E.: "General Purpose Compositional Model," *Soc. Pet. Eng. J.*, Vol. 25, No. 4 (1985) 543-553.

Afidick, D., Kaczorowski, N.J., and Bette, S.: "Production Performance of a Retrograde Gas Reservoir: A Case Study of the Arun Field," paper SPE 28749 presented at the SPE Asia Pacific Oil and Gas Conference, Melbourne, Australia, Nov. 7-10, 1994.

Burger, J.E. and Mohanty, K.K.: "Mass Transfer from Bypassed Zones During Gas Injection," *SPE Reservoir Engineering*, 124-130 (May 1997).

Burger, J.E., Spingate, G.S., and Mohanty, K.K.: "Experiments on Bypassing During GasFloods in Heterogeneous Porous Media," *SPE Reservoir Engineering*, 109 (May 1996).

Carman, P.C., "Fluid Flow Through a granular bed," Transactions of the Institution of Chemical Engineering, London, Vol. 15, 150-167 (1937).

Chang, Y.B., G.A. Pope, and K. Sepehrnoori: "A Higher-Order Finite Difference Compositional Simulator," *J. Pet. Sci. Eng.*, 5 (1990) 35-50.

Henderson, G.D., Danesh, D.H., Tehrani, S.I, Pantling, J. and Al-Shaidi, S.: "Gas Condensate Recovery Project," *Progress Report August-December 96*, Heriot-Watt University, UK, 1997.

Nghiem, L.X., and Sammon, P.H., "A non-Equilibrium Equation-of-State Compositional Simulator," paper SPE 37980 presented at the 1997 SPE reservoir Simulation Symposium, Dallas TX, June 8-11.

Peng, D.-Y. and Robinson, D.B.: "A New Two-Constant Equation of State," Ind. Eng. Chem. Fundam., Vol. 15, No. 1 (1976) 59-64.

Reid, R.C., Prausnitz, J.M. and Poling, B.E. *The properties of Gases and Liquids*, Forth edition, McGraw-Hill Inc., New York (1987).

Turek, E.A., Metcalfe, R.S., Yarborough, L., and Robinson, R.L.: "Phase Equilibria in CO2-Multicomponent Hydrocarbon Systems: Experimental Data and An Improved Prediction Technique," *Soc. Pet. Eng. J.*, Vol. 24, No. 3 (1984) 308-324.

Twu, C.H.: "An Internationally Consistent Correlation for Predicting the Critical Properties and Molecualr Weights of Petroleum and Coal-Tar-Liquids," *Fluid Phase Equilibria*, 16 (1984) 137.

Wang, P., Pope, G.A. and Sepehrnoori, K. "Development of Equation of State for Near Critical Gas Condensates," Submitted to Ind. & Eng. Chem. Research (1997).

Wilke, C.R.: "Diffusional Properties of Multicomponent Gases," *Chem. Eng. Progress*, 95 (1955).

Wilke, C.R. and Chang, P.: *AICHE J.* 1:264 (1955)

Wilke, C.R. and Lee, C.Y.: *Ind. Eng. Chem.*, 47:1253 (1955)

Wilkins, M.D., L.M. Abriola, and K.D. Pennell: "An Experimental Investigation of Rate-limited Nonaqueous Phase Liquid Volatilization in Unsaturated Porous Media: Steady State Mass Transfer," water resources research, vol. 31, no. 9, 2159-2172 (Sept. 1995).

Appendix A: Calculation of the diffusion coefficients

Wilke and Lee (1955) correlation:

$$D_{AB} = \frac{\left[3.03 - (0.98/M_{AB}^{1/2})\right] 0^{-3} T^{3/2}}{P M_{AB}^{1/2} \sigma_{AB}^2 \Omega_D}$$

Where
T = temperature, k
M_A, M_B = molecular weights of A and B, g/mole
$M_{AB} = 2[(1/M_A)+(1/M_B)]^{-1}$
P = pressure, bar

$$\sigma = 1.18 V_b^{1/3}$$

where V_b = liquid molar volume, cm^3/mole

$$\Omega_D = \frac{A}{(T^*)^B} + \frac{C}{\exp(DT^*)} + \frac{E}{\exp(FT^*)} + \frac{G}{\exp(HT^*)}$$

with $T^* = T/(\xi/k)_{AB}$

where A = 1.06036 B = 0.15610
C = 0.19300 D = 0.47635
E = 1.03587 F = 1.52996
G = 1.76474 H = 3.89411
$(\xi/k)_{AB} = 1.15Tb$
T_b = the normal boiling point (at 1 atm), k

The Wilke-Chang Correlation (1955) :

$$D_i = \frac{7.4\times10^{-8}(M_i')^{1/2} T}{\mu_o v_{bi}^{0.6}}$$

with $$M_i' = \frac{\sum_{j \neq i} x_{jo} M_j}{1 - x_{io}}$$

$$v_{bi} = 0.285 V_c^{1.048}$$

where μ_o = oil phase viscosity,
v_{bi} = volume of component i at T_b.
V_c = critical volume

Table 1. Description of the Gas Condensate.

Comp. name	z %	T_c K	P_c atm	V_c cm^3/mol	ω	Parachor
CO_2	16.18	304.2	72.8	93.90	0.225	49.0
C_1	70.98	190.6	45.4	99.20	0.008	71.0
C_{2-3}	7.90	330.5	45.7	169.64	0.119	130.0
C_{4-6}	2.60	453.8	34.9	298.58	0.226	230.0
C_9	2.00	606.0	26.0	490.35	0.359	327.0
C_{22}	0.34	869.7	14.9	1058.94	0.788	761.0

Table 2. The Diffusion Coefficients (cm^2/sec) for Each Component

Component	Diffusion coefficient in oil phase ($x10^4$)	Diffusion coefficient in gas phase ($x10^4$)
CO_2	5.38	11.8
methane	6.23	15.0
ethane	4.30	9.17
propane	3.22	5.75
n-butane	2.78	4.46
n-pentane	2.49	3.47
n-undecane	0.879	1.53

Table 3. Reservoir Permeability and Porosity.

Layer	Thickness (ft)	Porosity (%)	Permeability (md)
1	10	0.300	90
2	10	0.250	75
3	30	0.214	50
4	50	0.220	28
5	100	0.209	12
6	50	0.219	17
7	150	0.127	2.6
8	370	0.120	1.5

Table 4. Injection Fluid Compositions

Component	Mole fraction
CO_2	0.16551
methane	0.72624
C_{2-3}	0.08072
C_{3-4}	0.02584
Plus1	0.011687

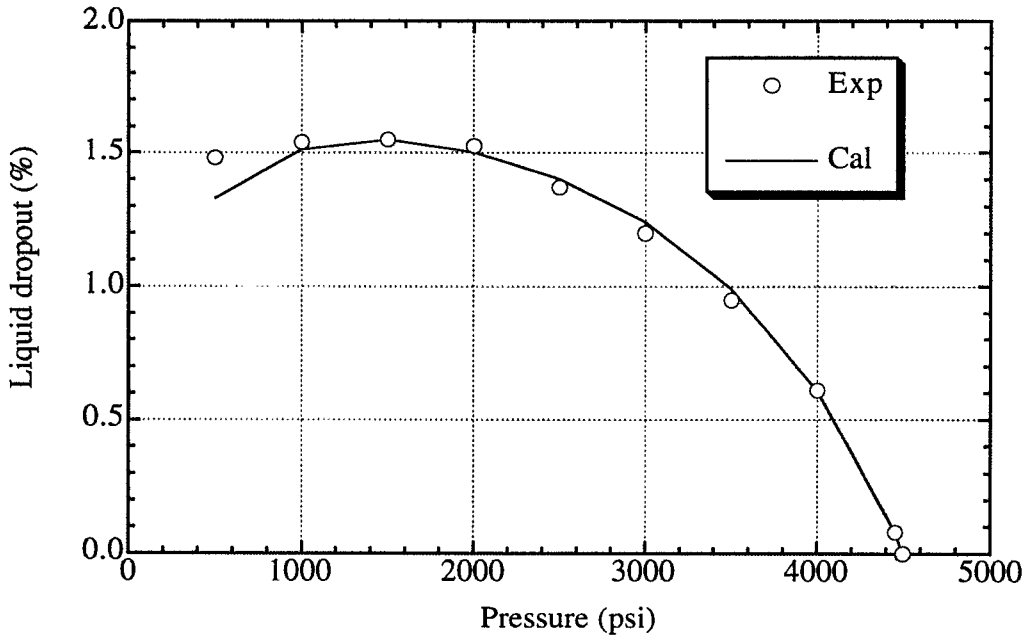

Figure 1. The liquid dropout curve using the 6-component PR EOS (T=352°F).

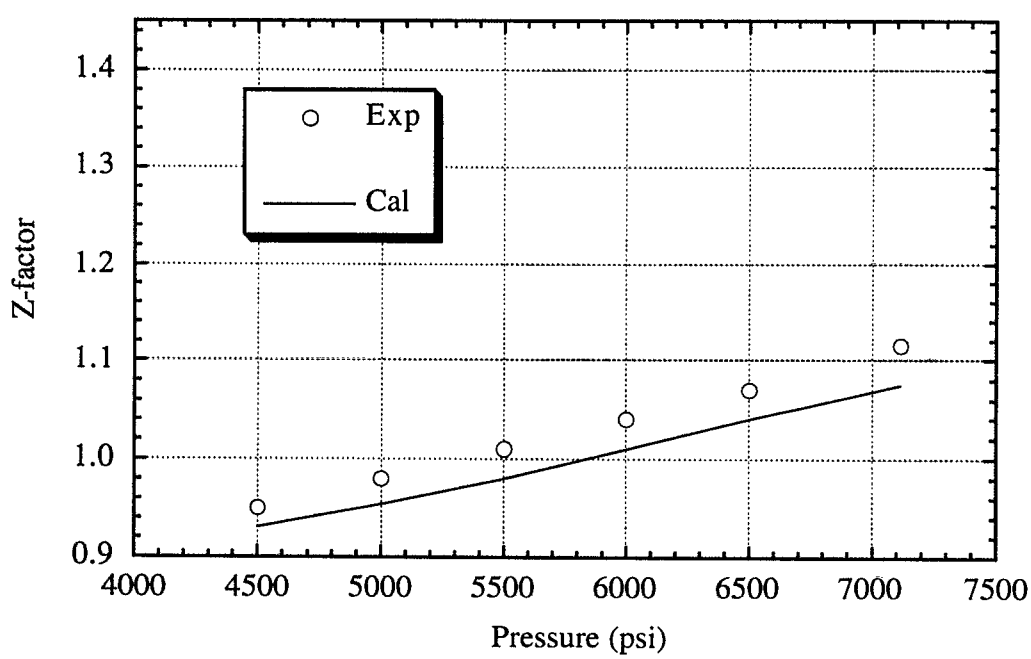

Figure 2. Z-factor from the 6-component PR EOS.

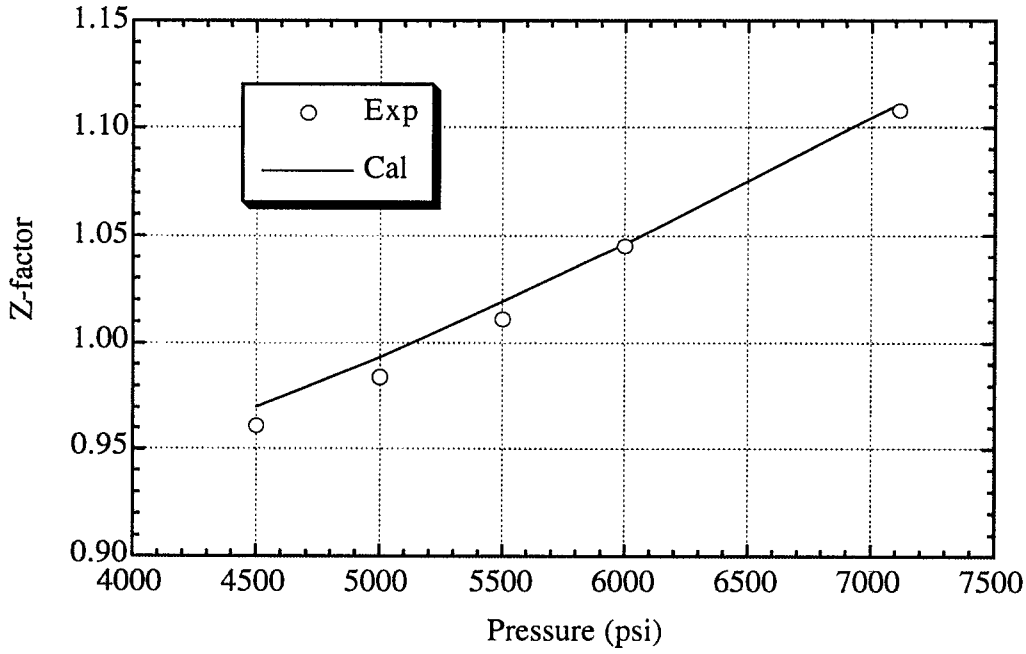

Figure 3. Z-factor for a wet fluid sample from the 6-component PR EOS.

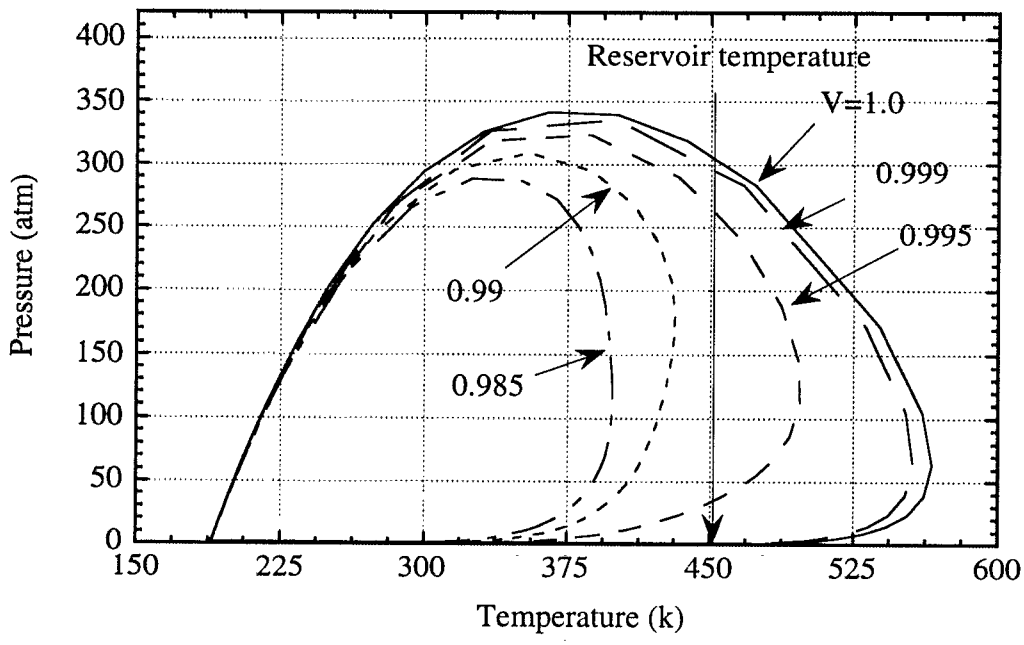

Figure 4. The phase envelop from the 6-component EOS.

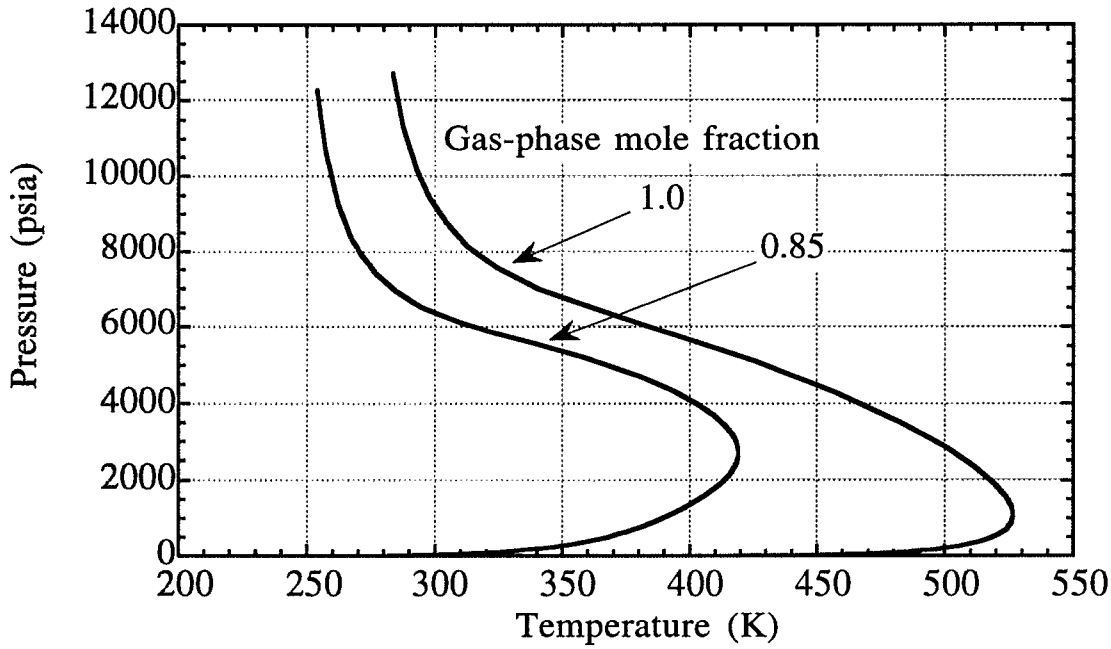

Figure 5. Phase envelope from a model of tuning the binary interaction coefficients.

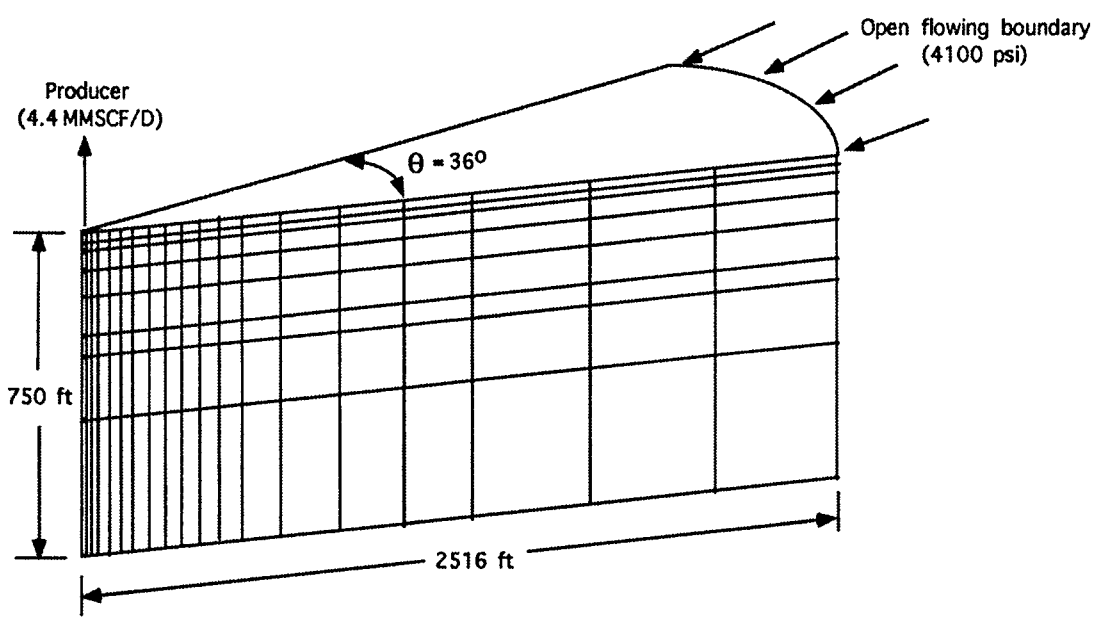

Figure 6. Schematic of grids used in the simulation study

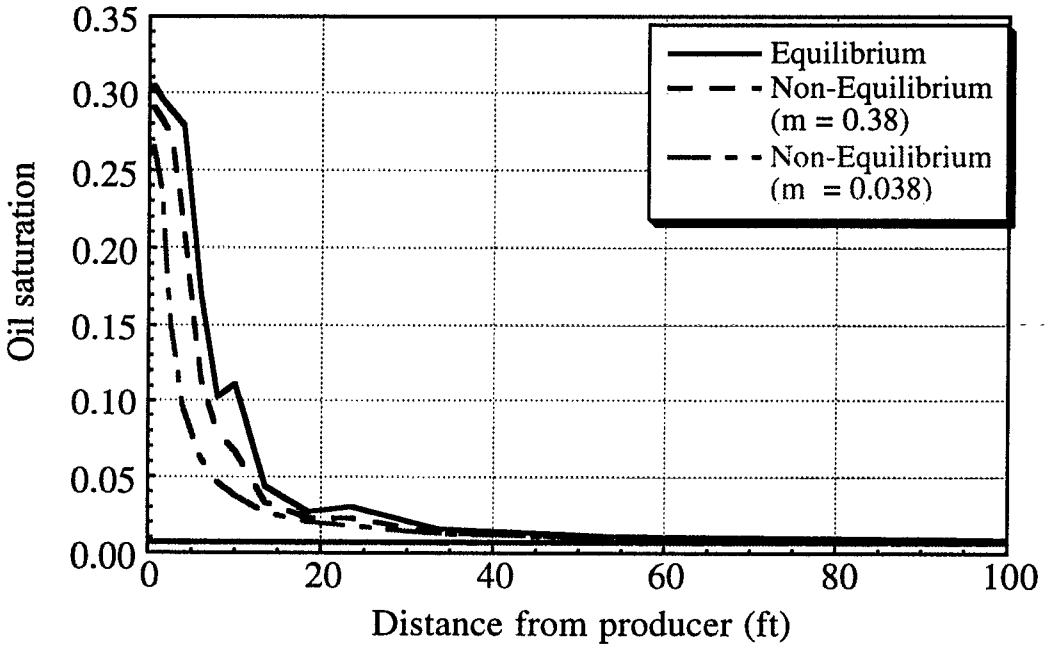

Figure 7. Effect of non-equilibrium mass transfer on oil saturation in layer 1 (Time = 10 days)

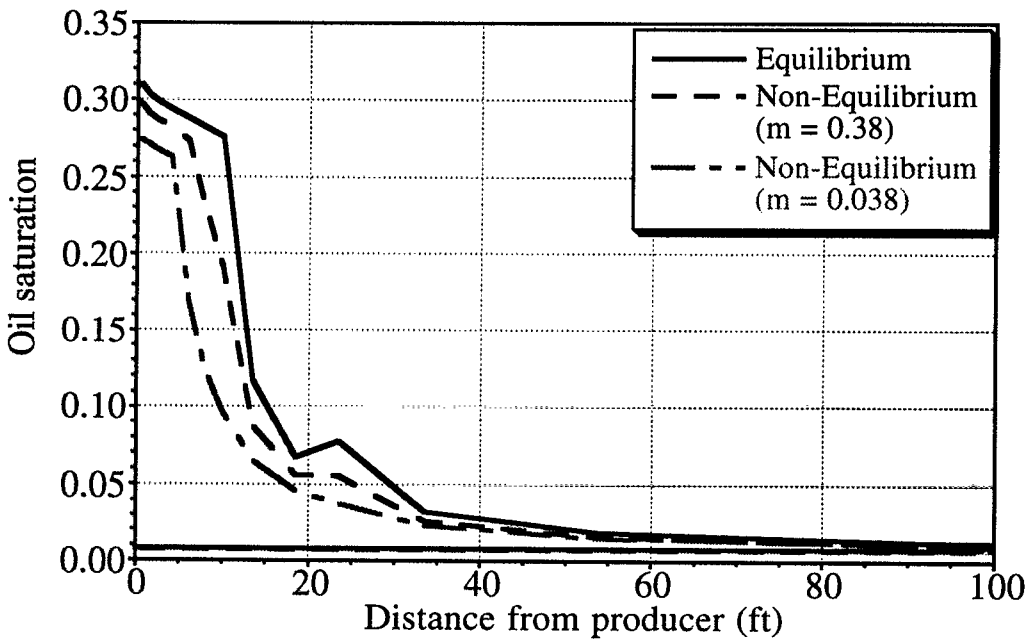

Figure 8. Effect of non-equilibrium mass transfer on oil saturation in layer 1 (Time = 30 days)

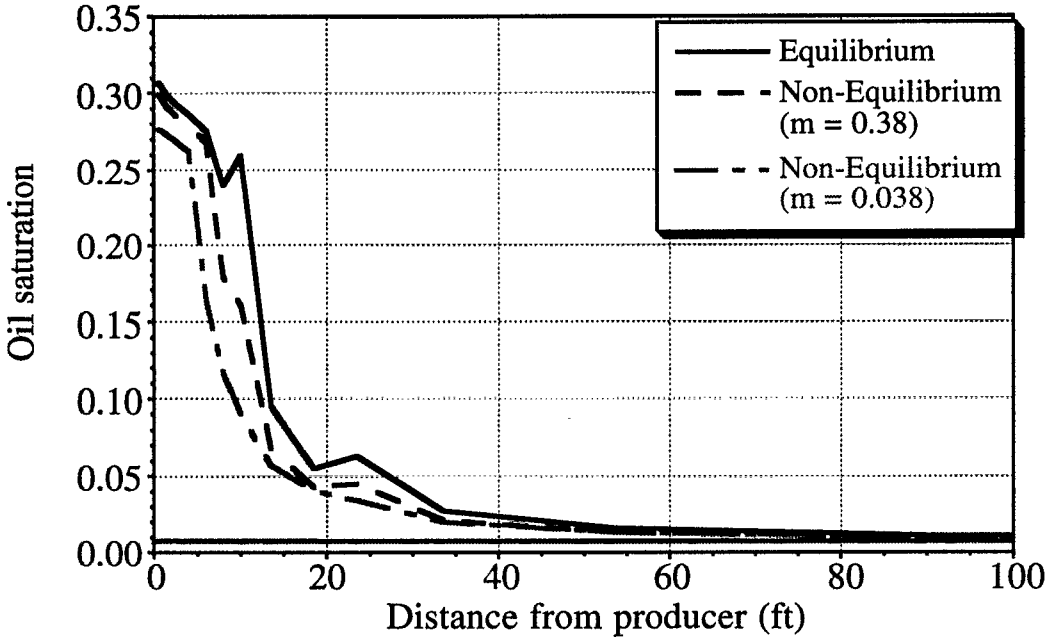

Figure 9. Effect of non-equilibrium mass transfer on oil saturation in layer 3 (Time = 30 days)

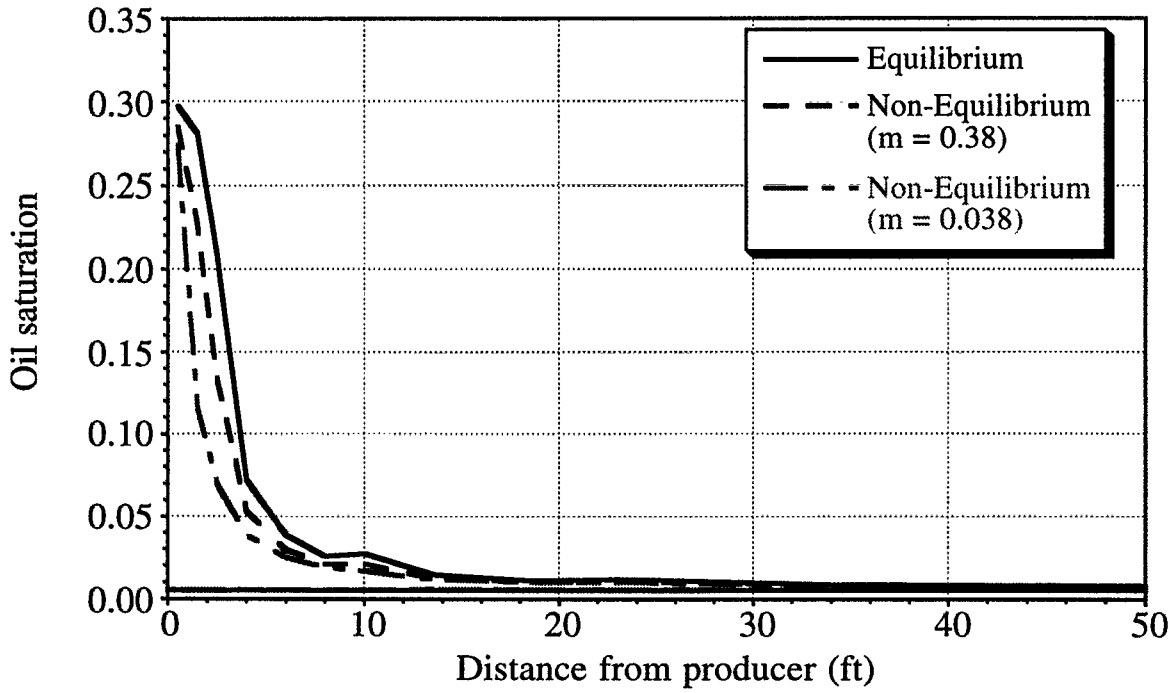

Figure 10. Effect of non-equilibrium mass transfer on oil saturation in layer 8 (Time = 30 days)

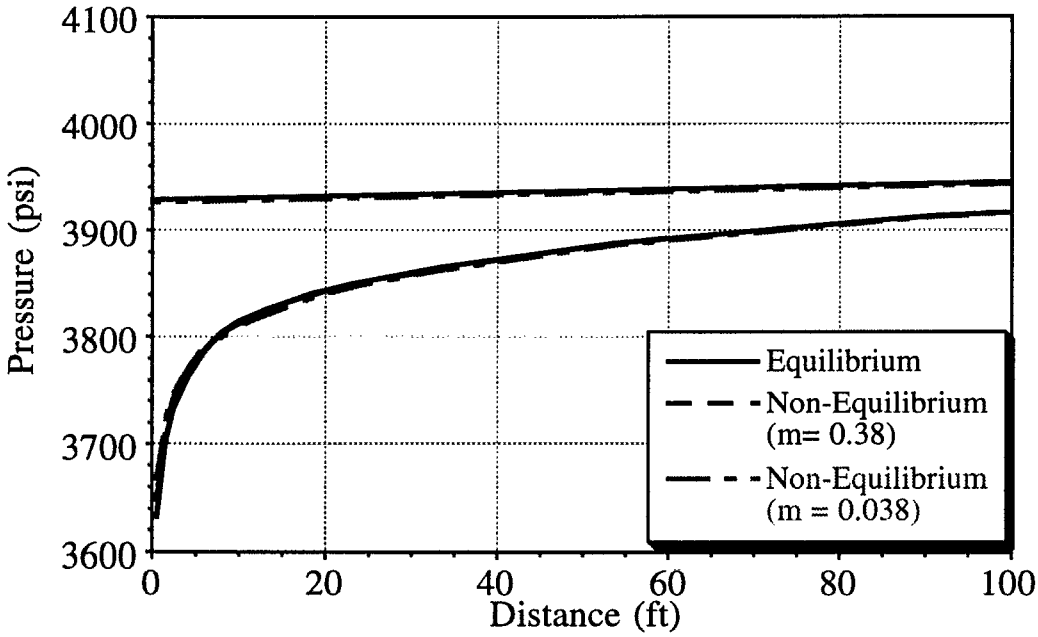

Figure 11. Effect of non-equilibrium mass transfer on presure distribution in layer 1 (Time = 30 days)

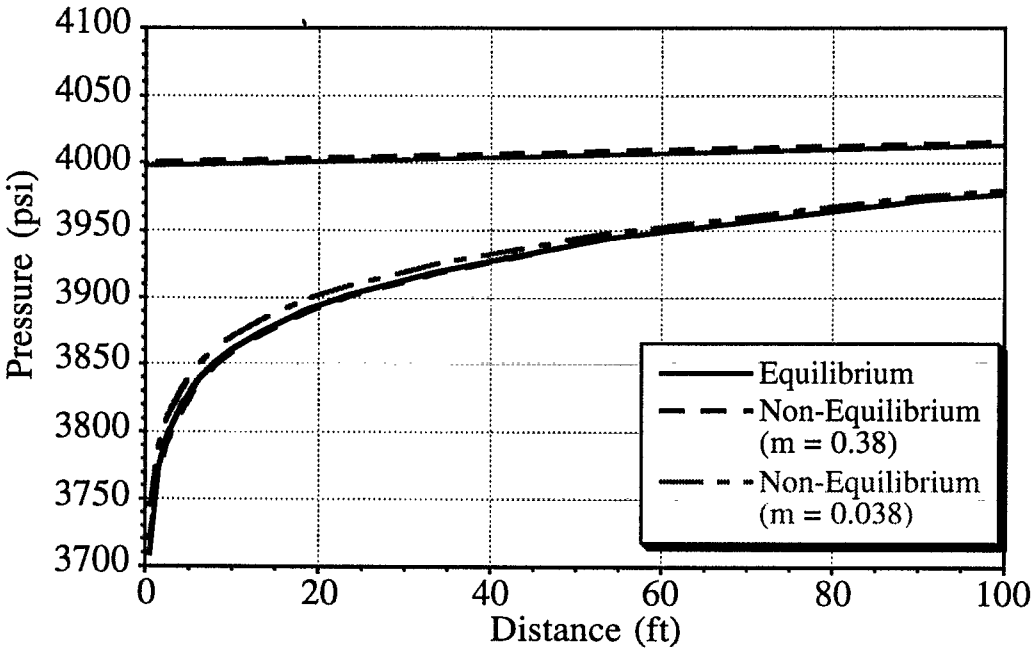

Figure 12. Effect of non-equilibrium mass transfer on presure distribution in layer 8 (Time = 30 days)

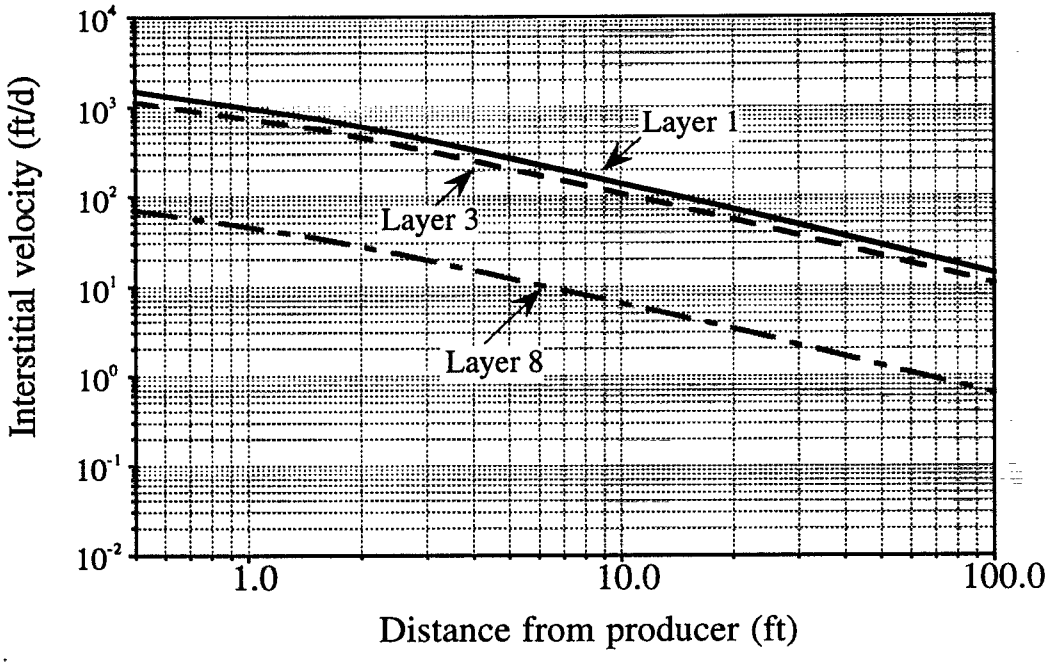

Figure 13. Gas phase interstitical velocity profiles at 30 days

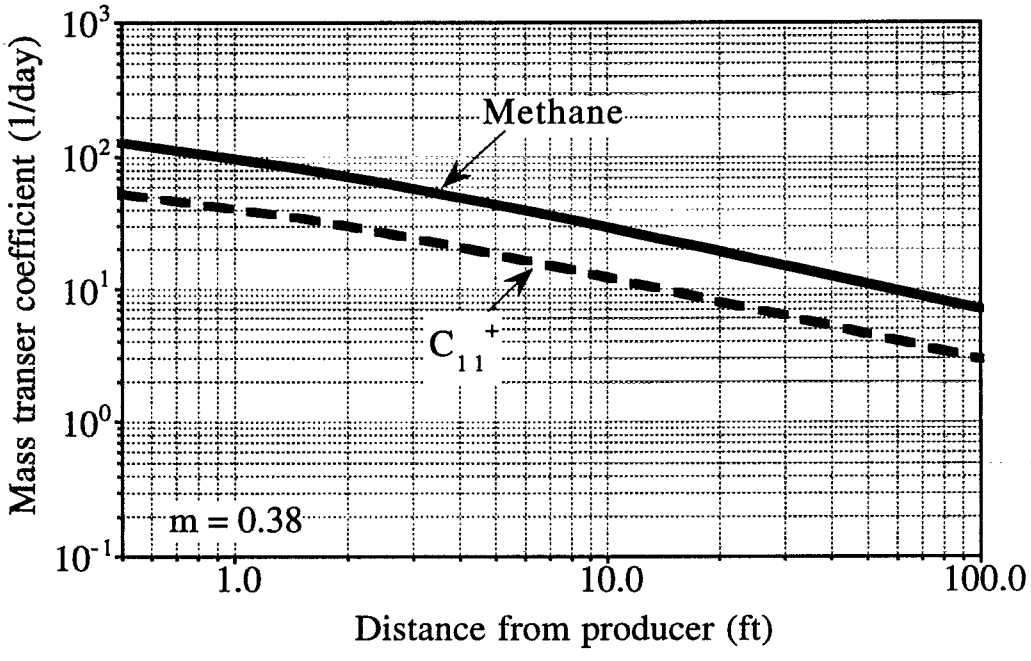

Figure 14. Mass transfer coefficient profiles in layer 1 at 30 days

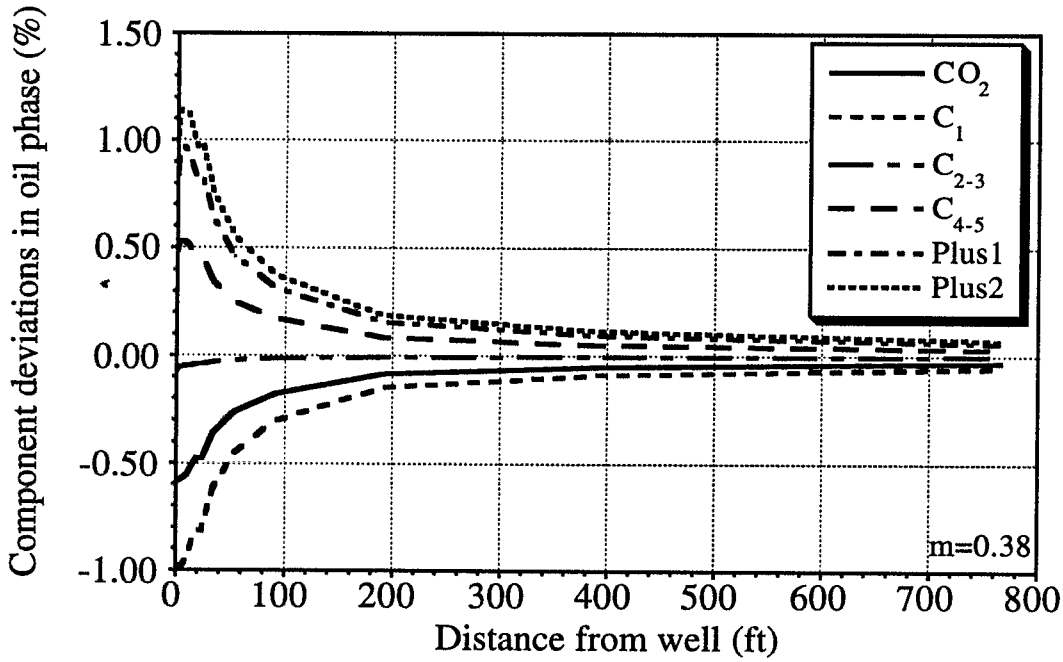

Figure 15. Effect of non-equilibrium mass transfer on component distributions in oil phase (Layer 1, Time = 30 days)

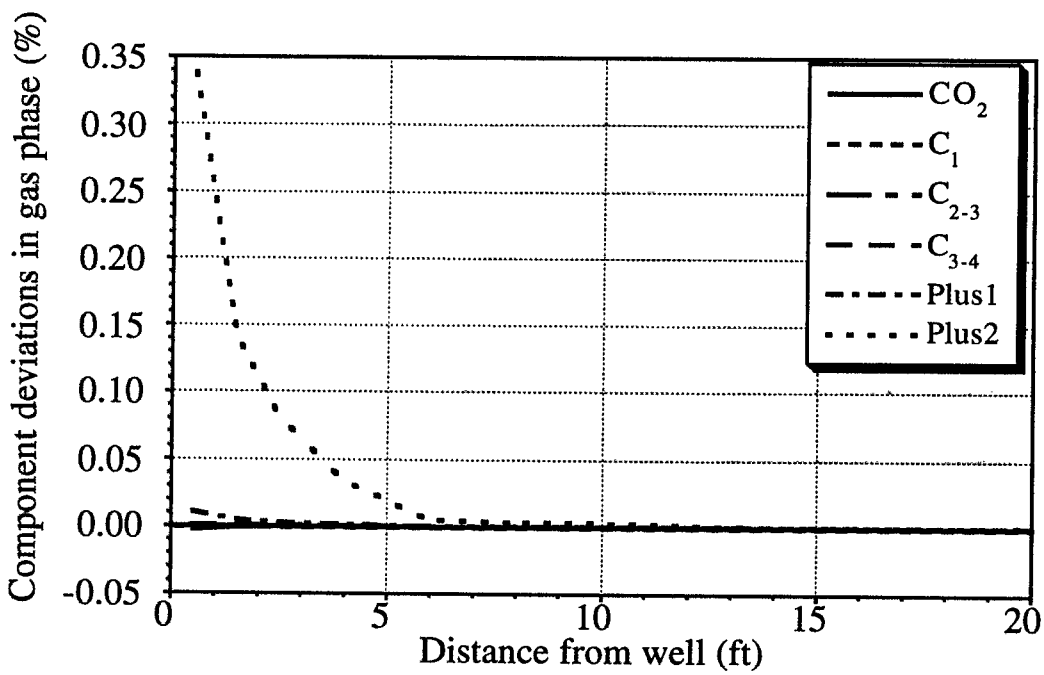

Figure 16. Effect of non-equilibrium mass transfer on component distributions in gas phase (Layer 1, Time = 30 days)

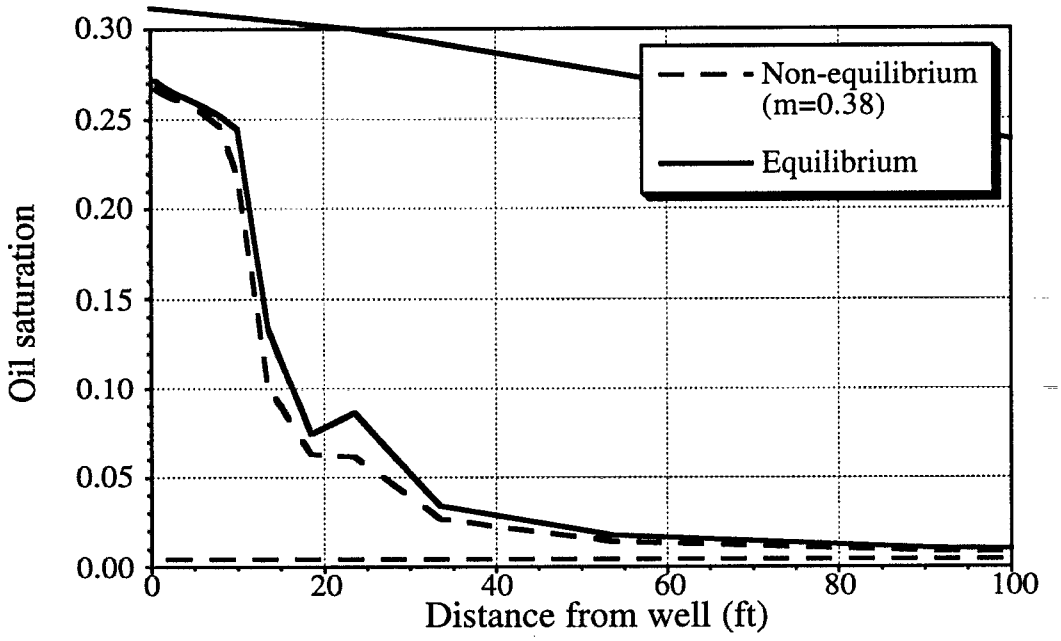

Figure 17. Effect of non-equilibrium mass transfer on oil saturation (Layer 1 , Time = 60 days)

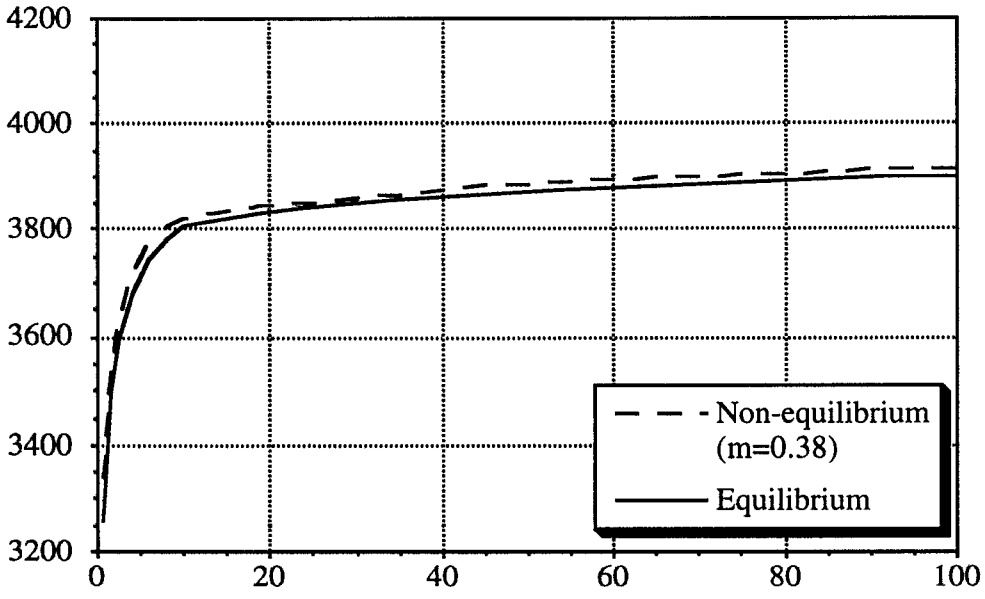

Figure 18. Effect of non-equilibrium mass transfer on pressure (Layer 1 , Time = 60 days)

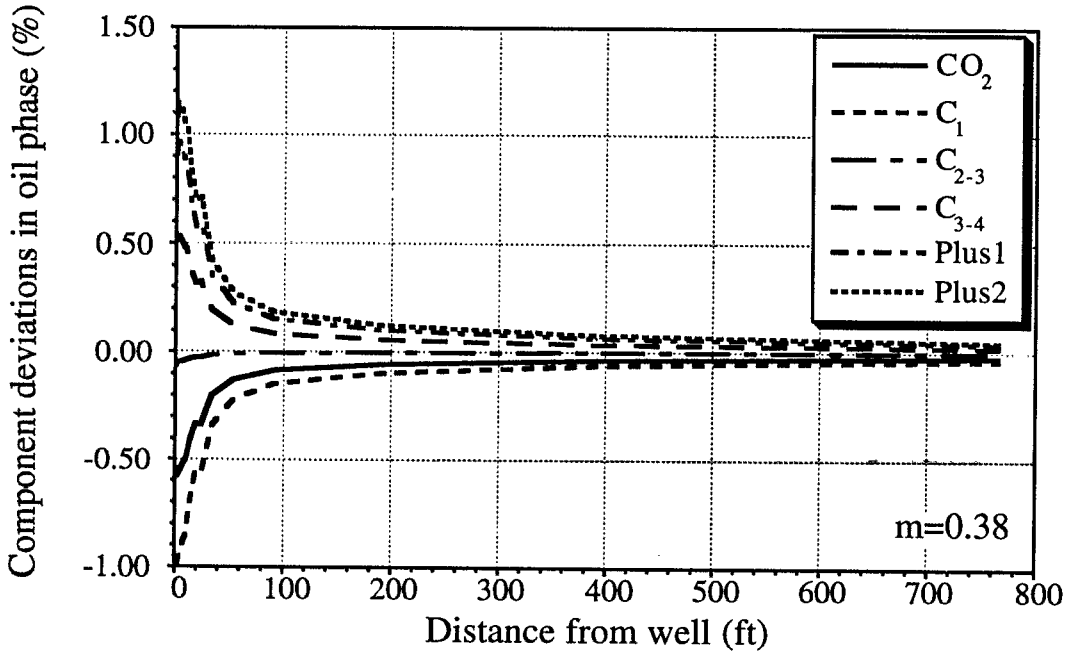

Figure 19. Effect of non-equilibrium mass transfer on component distribution in oil for the gas injection case (Layer 1 at 10 days)

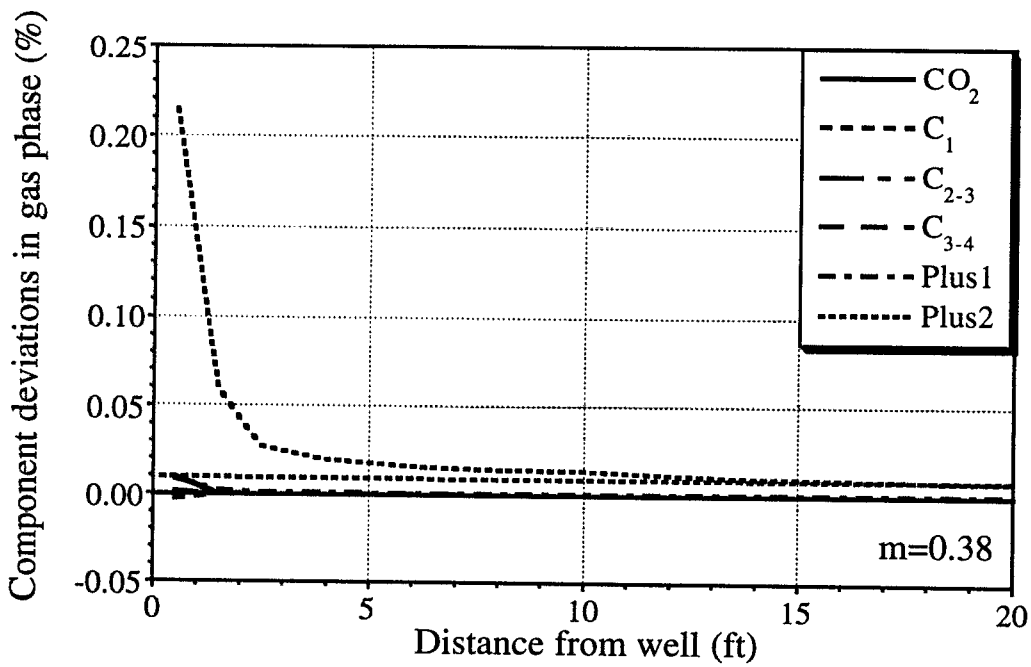

Figure 20. Effect of non-equilibrium mass transfer on component distribution in gas for the gas injection case (Layer 1 at 10 days)